Geophys. J. Int. (2005) **160,** 477–486 doi: 10.1111/j.1365-246X.2004.02493.x

Rock magnetic properties of remagnetized Palaeozoic clastic and carbonate rocks from the NE Rhenish massif, Germany

A. Zwing, J. Matzka, V. Bachtadse and H. C. Soffel

Department for Earth and Environmental Sciences, Geophysics section, LMU München, Theresienstr. 41, 80333 *München, Germany.*
E-Mail: azwing@geophysik.uni-muenchen.de

Accepted 2004 September 27. Received 2004 September 8; in original form 2002 August 5

SUMMARY

Several rock magnetic properties are reported for remagnetized biohermal carbonate rocks, platform carbonate rocks and siliciclastic rocks from the NE Rhenish massif, Germany. Thermal demagnetization of a triaxial isothermal remanent magnetization (IRM) applied at room temperature identifies a variety of magnetic minerals in the sample set. Magnetite is the predominant magnetic phase and carries a Late Palaeozoic remagnetization component and can be accompanied by haematite and pyrrhotite as the carrier of remagnetization. High haematite contents are characteristic for samples carrying a remagnetization of Triassic age. Zero field heating of remanence acquired at 10 K indicates significant contribution from magnetic material with blocking temperatures between 10 and 100 K. The Verwey transition at 120 K is much more pronounced in siliciclastic rocks than in carbonate rocks and is presumably related to the presence of detrital multidomain (MD) magnetite. Samples from biohermal carbonate rocks have hysteresis properties with high M_{rs}/M_s and H_{cr}/H_c ratios similar to those from remagnetized carbonate rocks from North America. In those lithologies, the intensity decrease of a low temperature IRM during heating from 10 to 100 K combined with the absence of paramagnetic minerals, high hysteresis ratios, magnetic viscosity and frequency dependence of susceptibility give strong evidence for the presence of superparamagnetic (SP) magnetite. This supports the hypothesis of a chemical remagnetization event in the NE Rhenish massif during the Late Carboniferous. The rock magnetic properties of siliciclastic rocks are characterized by high amounts of paramagnetic material and MD magnetite. MD material obscures the contributions of other material to the bulk magnetic properties completely in most siliciclastic rocks and partly in platform carbonate rocks.

Key words: Carboniferous, crystallization remanent magnetization, palaeomagnetism, remagnetization, rock magnetism, sedimentary rocks.

1 INTRODUCTION

Many palaeomagnetic studies of the last decades have presented evidence for a widespread remagnetization event during the Permo-Carboniferous reversed superchron (e.g. McCabe & Elmore 1989; Elmore *et al.* 1993; McCabe & Channell 1994; Molina Garza & Zijderveld 1996; Stamatakos *et al.* 1996; Zegers *et al.* 2003). During this event, the primary magnetization of numerous Palaeozoic rock units was partly or completely overprinted by a secondary magnetic component. At present, two different processes are thought to be responsible for remagnetization of large volumes of rock: (i) regional metamorphism, resulting in elevated palaeotemperatures and causing a thermoviscous magnetization or (ii) chemical processes, promoting the alteration of existing or the formation of new magnetic material, which may acquire a magnetization in the direction of the ambient magnetic field. While high palaeotemperatures are reflected in several petrophysical properties (like mineral thermometers, conodont alteration index, vitrinite reflectance and illite crystallinity), the identification of authigenic magnetic material resulting from chemical alteration relies on observations with electron microscopes and rock magnetic measurements.

An early and common observation in scanning electron microscopy (SEM) of remagnetized carbonate rocks of North America is the presence of magnetite spherules with diameters in the range of several tens of μm (e.g. McCabe & Elmore 1989). Although presumably a product of authigenic processes, the spherules have multidomain (MD) magnetic characteristics and are unlikely to carry stable ancient magnetizations (Xu *et al.* 1994). However, high-resolution scanning transmission electron microscopy (STEM) studies on magnetic extracts from remagnetized carbonate rocks revealed very fine grained magnetite (*ca* 200 nm) in the Single-Domain (SD) and Pseudo-Single-Domain (PSD) grain size range, which is authigenic in origin (Suk *et al.* 1991, 1993). Rock magnetic studies on these rocks (Jackson 1990; Jackson *et al.* 1993) yield a combination of particular rock magnetic properties (e.g. high frequency dependence of susceptibility k_{fd}; high ratios of both ferromagnetic susceptibility to saturation magnetization k_f/M_s and anhysteretic remanence magnetization to saturation isothermal remanence magnetization, ARM/SIRM), which reflect a significant contribution of even smaller, ultrafine particles with superparamagnetic (SP) properties. These particles are thought to result from the same authigenic processes as the more readily observable larger particles (Jackson *et al.* 1993). Unusually high hysteresis ratios [$M_{rs}/M_s = 0.89\ (H_{cr}/H_c)^{-0.6}$] indicate a mixture of SD magnetite dominated by magnetocrystalline anisotropy and ultrafine SP magnetite (Jackson 1990), but could also be caused by mixtures of magnetite and pyrrhotite (Jackson *et al.* 1993). Similar hysteresis properties were observed in remagnetized Palaeozoic carbonate rocks from Alaska, northern England (McCabe & Channell 1994) and the Brabant and Ardennes massifs, Belgium (Molina Garza & Zijderveld 1996). Although interpretations are not unequivocal, the unusual hysteresis properties have been suggested to be diagnostic for remagnetization in carbonate rocks (McCabe & Channell 1994).

A palaeomagnetic study (Zwing *et al.* 2002) on siliciclastic and carbonate rocks from the NE Rhenish massif identified a widespread secondary magnetization, which is mainly carried by magnetite and which has been acquired during the main deformation phase in the Late Carboniferous. The combination of low to moderate palaeotemperatures (Königshof 1992; Paproth & Wolf 1973) and high laboratory unblocking temperatures of the remagnetization component favour a chemical remagnetization process. A younger remagnetization of Triassic age affected rocks more locally in zones of tight folding with steeply dipping to overturned bedding planes. The present study was designed to identify the remanence carrying minerals in a variety of remagnetized sedimentary lithologies from the NE Rhenish massif and to test whether the characteristic hysteresis properties of remagnetized carbonate rocks can be identified. Additionally, a series of rock magnetic experiments (magnetic viscosity, k_{fd}, low temperature behaviour) was carried out in order to identify any possible contribution of ultrafine magnetic (SP) particles to the bulk magnetic properties.

2 SAMPLES

The sedimentary basin of the Rhenish massif evolved from shallow marine and deltaic conditions on the southern shelf of the Old Red Continent in Early Devonian times. The Lower and Middle Devonian sequences are characterized by thick clastic deposits and the occurrence of red beds, root horizons and conglomerates. During subsidence of the shelf, the neritic facies gave way to hemipelagic and pelagic environments in Middle and Late Devonian times. Bioherms, which developed in the photic zone on top of submarine seamounts with heights of a few hundred metres indicate the relatively shallow depth of the basin. A trangressive event at the Devonian–Carboniferous boundary almost completely terminated the clastic sedimentation and led to the formation of a carbonate platform further to the north. At the same time, the closure of the Rhenohercynian basin caused the formation of a flysch trough, which propagated northwestwards during the Early Carboniferous (Walliser 1981; Franke 2000).

The sedimentary rocks of the Rhenish massif can be subdivided into three major groups: (i) siliciclastic rocks deposited in neritic to pelagic environments; (ii) carbonate rocks deposited on the Late Devonian/Early Carboniferous carbonate platform; and (iii) carbonate rocks formed in the vicinity of bioherms. Widespread occurrence and large thickness of siliciclastic sediments are characteristic for the Rhenish massif, while outcrops of Late Devonian and Early Carboniferous carbonate rocks are restricted to large synclinal structures and a narrow zone in the northern part of the basin. Consequently, the majority of the samples studied were taken from siliciclastic lithologies. Samples from four localities each represent biohermal and platform carbonates. The lithologies of the samples studied are given in Table 1.

The siliciclastic rocks comprise mainly of quartzwackes and lithic greywackes (Pettijohn *et al.* 1973) and contain significant amounts (>15 per cent) of silt-grade quartz and clay minerals. X-ray diffraction (XRD) studies of the <2 μm grain size fractions identify illite/sericite and Fe-chlorite as the main clay minerals. The lithic clasts are often altered and replaced by clay minerals (sericite, chlorite). Only a few sandstones (quartzarenites) have no or little amounts of matrix. The grain sizes of the majority of siliciclastic rocks fall in the range of fine grained sandstones. While coarser lithologies are rare, several samples are finer grained siltstones. The occurrence of plant fragments and the dark grey colours of most siliciclastic rocks indicate anoxic to suboxic conditions during sedimentation and early diagenesis. Only in samples from the Lower Devonian red beds (site PLE), does field and microscopic evidence indicate the sedimentary or early diagenetic nature of haematite.

The platform carbonate rocks are commonly biomicrites and oomicrites (Folk 1957), which can contain significant amounts of biogenic material. Carbonate build-ups (bioherms) are mainly formed by authochtonous biolithites and dolodismicrites (Folk 1957). All carbonate rocks are characterized by low amounts of clay minerals and the absence of chlorite.

The different amounts of clay minerals such as chlorite in the three groups of lithologies are thought to reflect differences in the amount of terrigeneous detritus. While predominant and relatively coarse in siliciclastic rocks, the amount and grain size of terrigeneous material is greatly reduced in the platform carbonate rocks and almost absent in carbonate rocks from bioherms. Because terrigeneous detritus is an important source of ferromagnetic minerals (e.g. magnetite), paramagnetic minerals (micas, Fe-chlorite) or their precursors (mafic minerals, lithic clasts), the rock magnetic properties of the studied rocks can be expected to be similar within each group of lithologies, in the following referred to as siliciclastic rocks, platform carbonate rocks and biohermal carbonate rocks.

3 METHODS

Stepwise thermal demagnetization and the measurement of the natural remanent magnetization (NRM) of palaeomagnetic specimens (11 cm^3) was carried out using a 2G Enterprises DC-SQUID magnetometer and two Schonstedt TSD-1 furnaces in a magnetically shielded room in the palaeomagnetic laboratory of the University of Munich. The same instruments were used to measure the acquisition of an isothermal remanent magnetization (IRM) with a Magnetic Measurements Pulse Magnetiser (MMPM9) and the thermal demagnetization behaviour of a three component IRM at 0.12, 0.4 and 2.6 T (Lowrie 1990). All other measurements were carried out at the Institute for Rock Magnetism, University of Minnesota. The hysteresis parameters of specimens, 11 cm^3 in volume, were measured with a Vibrating Sample Magnetometer (VSM, Princeton Measurements). The VSM was also used to determine the ferromagnetic susceptibility from hysteresis loops and the magnetic viscosity by continuous monitoring an IRM (1T) of a sample for 290 s. This time was chosen as a reasonable relaxation time for identification of grains near the SD–SP threshold. Before starting the measurement, the electromagnet of the VSM was given 10 s to stabilize down after IRM acquisition. Smaller specimens (mini drill cores, *ca* 0.2 cm^3

Table 1. Hysteresis parameters (Hcr, M_{rs}/M_s, H_{cr}/H_c), normalized magnetic viscosity coefficient [S/Mr(10s)], relative decrease in magnetization at the Verwey transition $\{\delta_{ZFC} = [M(100\,K)\text{-}M(130\,K)]/M(100\,K)\}$ and lithologies of the samples studied. The letters h, g and p indicate the occurrence of haematite, goethite or phyrrhotite. Magnetite is present in all samples and is the main carrier of the Late Carboniferous remagnetization (component B in Zwing *et al.* 2002). The Triassic remagnetization (component C in Zwing *et al.* 2002) resides in haematite.

Sample	H_{cr} (mT)	M_{rs}/M_s	H_{cr}/H_c	$S/M_r(10s)$ (s^{-1})	δ_{ZFC}		Lithology
Late Carboniferous remagnetization (component B)							
Biohermal carbonate rocks							
GRU1	38.5	0.29	4.81	0.027	0.12		Biolithite
NOR1-5	—	—	—	0.030	0.15	g, p	Dolodismicrite
STC1-1	74.3	0.15	20.9	0.032	0.15		Dolodismicrite
WES1-4	64.4	0.42	3.83	0.025	0.15		Biosparite
Platform carbonate rocks							
HAC2-2	37.6	0.08	9.40	—	—	p	Bitum. biomicrite
HAC2-3	37.9	0.07	12.0	0.021	0.14	p	Bitum. biomicrite
HEN1-2	53.5	0.03	27.0	0.032	—		Oomicrite
HEN1-5	—	—	—	—	0.33	g	Oomicrite
LET2-5	37.1	0.05	19.9	0.054	0.21	p	Cherty oomicrite
STU1-1	38.5	0.03	23.1	0.026	0.19		Oomicrite
Siliciclastic rocks							
ALB1-5	70.3	0.02	13.4	—	—		Siltstone
ALB1GM	56.5	0.06	9.50	—	0.38	p	Siltstone
ALB2-9	48.6	0.04	7.00	0.012	0.51		Siltstone
AMB1-5	120	0.06	12.5	0.015	—	p	Quartzwacke
ATT1-1	—	—	—	0.025	0.15	h	Quartzarenite
BOH1-14	141	0.04	21.4	0.007	0.42	p	Quartzarenite
BOH1-3	123	0.02	24.6	0.008	0.31	p	Quartzarenite
BRU1-6	50.6	0.04	8.28	0.020	0.24		Quartzwacke
BRU2-10	62.4	0.06	5.83	0.023	0.24		Quartzwacke
DOT2-7	109	0.03	12.8	0.006	—	p	Quartzwacke
ELV1-9	61.1	0.03	11.3	0.008	0.21	p	Siltstone
FIN1-8	47.0	0.01	15.3	0.026	0.62		Siltstone
HAM1-2	68.9	0.04	11.8	0.015	0.24		Quartzwacke
LAS1-1	52.5	0.05	6.69	—	0.37		Quartzarenite
LOS2-2	68.5	0.07	6.40	0.020	0.17	p	Quartzwacke
LOS3-4	85.1	0.15	5.67	0.018	—		Quartzwacke
MET1-5	56.5	0.05	8.55	0.011	—		Lithic greywacke
NEU1-4	56.2	0.10	4.43	0.010	—		Quartzarenite
OLP2-10	48.1	0.05	7.24	0.011	0.38	p	Lithic greywacke
PLE1-11	—	—	—	0.006	—	h	Red siltstone
PLE1-8	—	—	—	—	0.05	h	Red siltstone
PLE1-4	—	—	—	0.009	0.28	h	Rred quartzwacke
SOR3-7	63.8	0.05	7.18	0.028	—		Litharenite
Triassic remagnetization (component C)							
ATT1-1	—	—	—	0.025	0.15	h	Quartzarenite
ATT2-5	—	—	—	0.021	—	h	Red calcareous siltstone
ATT2-7	—	—	—	0.025	—	h	Red calcareous siltstone

in volume) were prepared for low temperature experiments (10–300 K) with a Magnetic Properties Measurement System (MPMS-XL5, Quantum Design). After acquisition of a 2.5 T IRM at 300 K, the samples were cooled to 10 K in zero field at a rate of 5 K min^{-1}. At 10 K another 2.5 T IRM was applied, the samples were then heated to 300 K at the same rate. The frequency dependence of the susceptibility (k_{fd}) of mini drill cores was measured using a Lakeshore Cryotronics susceptometer.

4 RESULTS AND INTERPRETATION

4.1 NRM demagnetization behaviour

During thermal and alternating field demagnetization, three components of magnetization can be identified in the sample set. In approximately 60 per cent of the specimens, a magnetization (component A in Zwing *et al.* 2002) is observed between 100 and 150 °C, which direction is similar to the present day field in the sampling area is observed. This magnetization is generally more prominent in specimens from siliciclastic rocks than in carbonate rocks and is thought to be a (thermo)viscous overprint of recent age. The Palaeozoic remagnetization (component B) is stable up to 550 °C, indicating that magnetite is its dominant carrier. However, in a few samples the unblocking temperature (T_{ub}) spectra suggest a combination of pyrrhotite and magnetite (T_{ub}: 320 and 550 °C) as the carriers of component B. In one locality from Lower Devonian red beds (site PLE), component B resides in magnetite and haematite (T_{ub}: 550–580 and 670 °C). In either case, a sharp decrease in intensity at low T_{ub} is not accompanied by a change in direction of the remanence vector (Zwing *et al.* 2002). A further remagnetization component of Triassic age (component C) is observed in specimens from Upper Devonian calcareous siltstones and quartzarenites. This

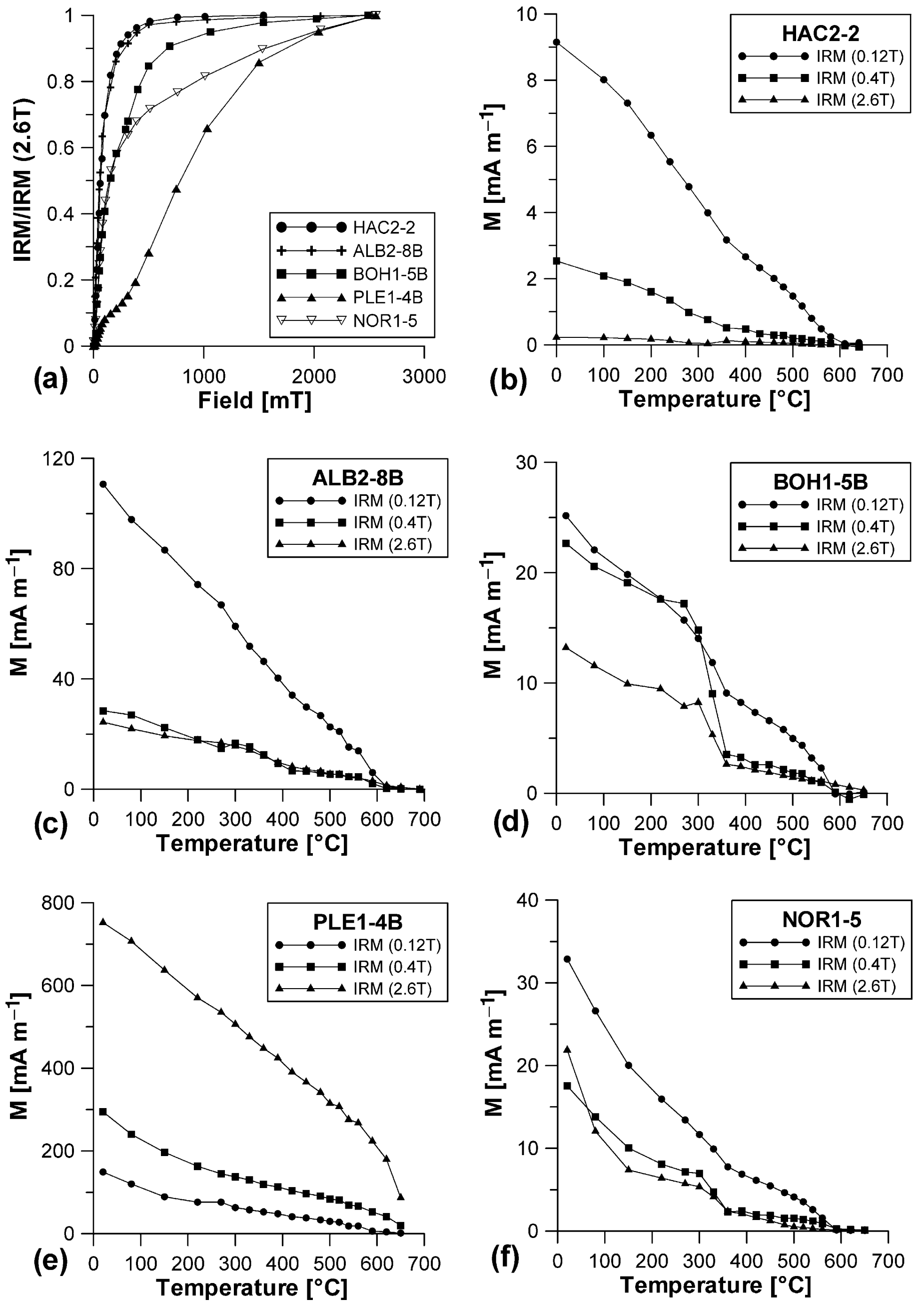

Figure 1. IRM acquisition (a) and thermal demagnetization of a triaxial IRM (0.12, 0.4, 2.6 T) of samples from (b) platform carbonate rocks (HAC2-2), (c) siltstones (ALB2-8B), (d) quartzarenites (BOH1-5B), (e) red siltstones (PLE1-4B) and (f) carbonate rocks (NOR1-5). Magnetite (T_c: 580 °C) appears to be present in all samples and is accompanied by pyrrhotite (T_c: *ca* 320 °C) in some siliciclastic rocks (BOH1-5B) and carbonate rocks (NOR1-5, HAC2-2) and by haematite (T_c: 670 °C) in red siltstones (PLE1-4B). In some carbonate rocks a significant portion of the high-coercivity component is demagnetized below 150 °C, indicating the presence of goethite (NOR1-5).

remagnetization component is exclusively observed within zones of tight folding and steep to overturned bedding planes and is characterized by unblocking temperatures up to 670 °C indicating haematite as the predominant carrier of this (re)magnetization. Here, the occurrence of haematite along fractures and fault zones in the cores of synclinal structures suggest the secondary nature of haematite.

4.2 IRM acquisition and demagnetization

Three characteristic behaviours of IRM acquisition were observed, indicating varying contributions of high-coercivity phases in the sample set (Fig. 1a). The majority of specimens reach saturation at fields around 0.5 T (HAC2-2 and ALB2-8B in Fig. 1a). Here, the low-coercivity component is most prominent and is removed at 600 °C, indicating the predominance of magnetite (Figs 1b and c). In platform carbonate rocks and siliciclastic rocks, magnetite can be accompanied by a phase interpreted as pyrrhotite, which is indicated by a decrease in intensity of the medium coercivity (0.12–0.4 T) component between 250 and 350 °C (Figs 1d and f). The field necessary to reach magnetic saturation of natural pyrrhotites is grain-size–dependent and varies between *ca* 0.25 and 2 T (Dekkers 1988). Therefore, the incomplete saturation at fields above 2 T

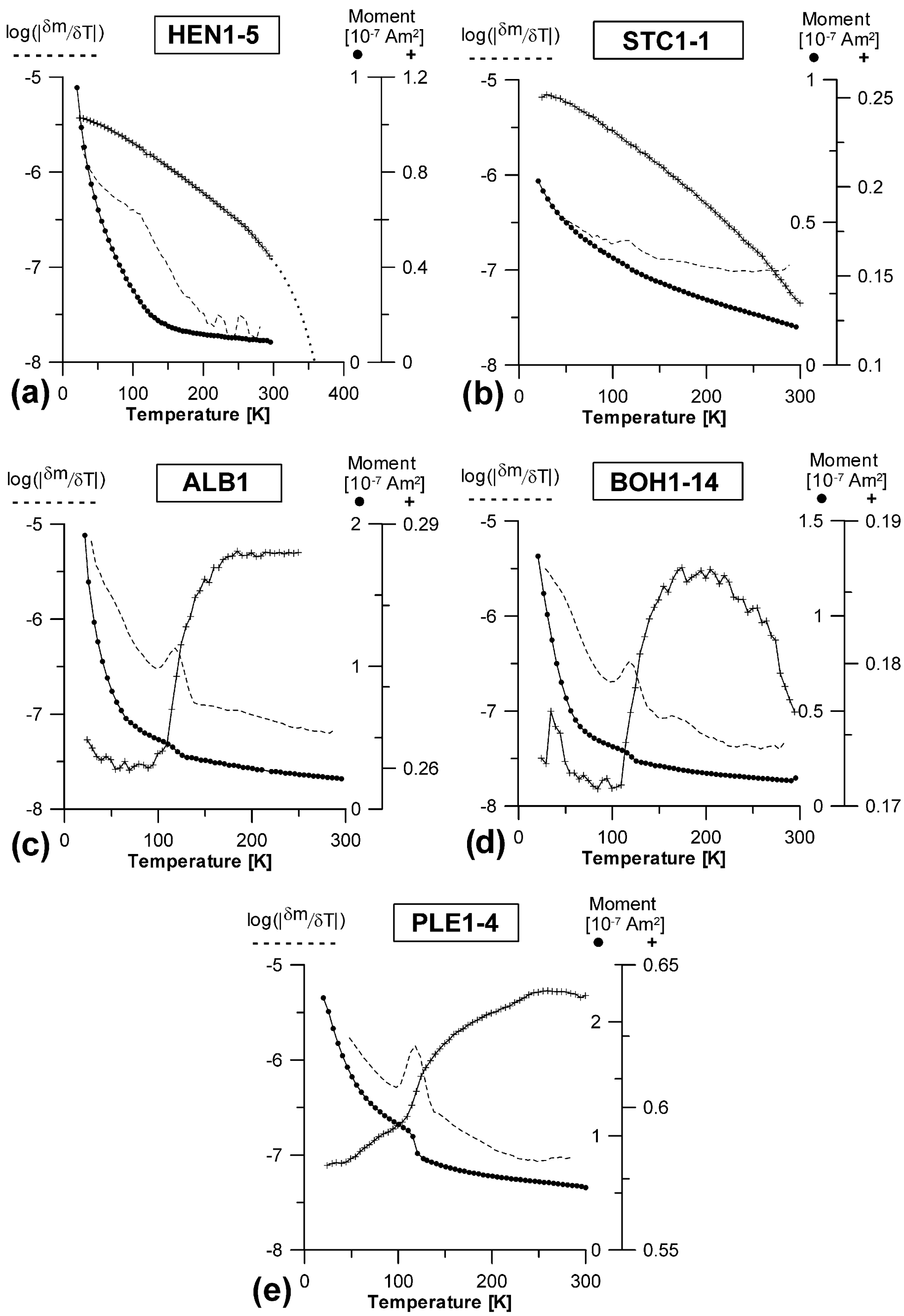

Figure 2. Low-temperature behaviour of (a) platform carbonate rocks (HEN1-5, dotted line is a qualitative estimate to higher temperatures), (b) reef carbonate rocks (STC1-1), (c) siltstones (ALB1), (d) quartzarenites (BOH1-14) and (e) red siltstones (PLE1-4). Thermal demagnetization of an IRM (2.5 T) acquired at 10 K and cooling of an IRM (2.5 T) acquired at room temperature is shown with circles and crosses, respectively. The dashed lines mark the first derivative of the zero field heating curve ($\log|\partial M/\partial T|$) and highlight the occurrence of the Verwey transition.

(BOH1-5B in Fig. 1a) is thought to be caused rather by goethite or haematite than by pyrrhotite. In samples from red siltstones, the IRM acquisition behaviour indicates the simultaneous presence of a low (<0.12 T) and high (>0.4 T) coercivity phase (PLE1-4B in Figs 1a and e). The low- and high-coercivity components are demagnetized at *ca* 580 and 670 °C, respectively, confirming the predominance of haematite, which is accompanied by magnetite (Fig. 1e). In some carbonate rocks, a distinct decrease in NRM and IRM (high-coercivity component) intensity is observed below 150 °C, which indicates the presence of goethite (Fig. 1f). The IRM demagnetization behaviour of samples carrying the Triassic remagnetization component is generally similar to that of sample PLE1-4.

4.3 Low temperature experiments

The results of the low temperature measurements for representative samples from different lithologies are shown in Fig. 2. Zero field cooling curves of an IRM_{RT} acquired at 300 K (2.5 T) down to 20 K (crosses in Fig. 2) and zero field heating curves of a low-temperature IRM_{LT} (2.5 T at 10 K after zero field cooling) from

20 to 300 K (circles in Fig. 2) were observed. Changes of the zero field heating curve are accentuated by the first derivative of the magnetic moment over temperature [$\log(|\partial M/\partial T|)$, dashed lines in Fig. 2].

All samples are characterized by a strong decrease of the zero field heating curve between 20 and 100 K. In carbonate rocks (HEN1-5, STC1-1, Figs 2a and b), this is generally thought to reflect the presence of SP magnetite with very low T_{ub}. In clastic rocks (ALB1, BOH1-14, PLE1-4, Figs 2c–e), however, this behaviour could also be caused by iron-bearing silicates, which are paramagnetic at room temperature, but magnetically order at very low temperatures (Coey 1988, and references therein). Similarly, the sharp increase of the zero field cooling curve below 30 K in samples ALB1 and BOH1-14 (Figs 2c and d) is probably caused by the combination of magnetic ordering and magnetic blocking in a small residual field within the MPMS (*ca* 0.1 mT).

Although T_{ub} observed during NRM demagnetization experiments (up to 550 °C, Zwing *et al.* 2002) indicate that the NRM is carried by magnetite in carbonate rocks, samples from those lithologies show only weak changes in magnetization at the Verwey transition, which can be identified by small peaks in the curves of derivatives (HEN1-5, STC1-1, Figs 2a and b). In contrast, a marked transition is observed during zero field heating of all siliciclastic rocks (ALB1, BOH1-14, PLE1-4, Figs 2c–e). The Verwey transition is also very well developed in the zero field cooling curves of the siliciclastic lithologies (crosses in Figs 2c–e). In general, the relative decrease in magnetization at the Verwey transition $\{\delta_{ZFC} = [\mathrm{M(100\ K)\text{-}M(130\ K)]/M(100\ K)}\}$ is smallest in biohermal carbonate rocks and largest in siliciclastic rocks (Table 1). The suppression of the Verwey transition in the magnetite-bearing carbonate rocks can be caused by either a very small SP particle size or by partly oxidized magnetite grains (Özdemir *et al.* 1993). Compared with the clastic lithologies, however, the carbonate rocks show no macroscopic or microscopic evidence for intensified oxidation. Consequently, non-stoichiometric, oxidized magnetite is not expected to be solely responsible for the low temperature behaviour of the carbonate rocks.

The presence of goethite in some carbonate rocks is evidenced by a continuous increase in the zero field cooling curve from 300 to 20 K (HEN1-5, crosses in Fig. 2a; Dekkers 1989a). However, the maximum blocking temperature estimated for sample HEN1-5 from a qualitative extrapolation of the zero field cooling curve to higher temperatures (dotted line in Fig. 2a) is approximately 360 K, which is lower than the Néel-temperature (393 K) of pure goethite. This difference could be explained by small amounts of isomorphous substitutions of Fe^{3+} by, for example, Al^{3+} in the crystal lattice of goethite (Dekkers 1989a).

The occurrence of pyrrhotite in the quartzarenites from site BOH is reflected in the sharp decrease in IRM intensity on cooling at the pyrrhotite transition temperature (32 K, Fig. 2d). The broad maximum between 150 and 200 K of the IRM intensity during cooling has also been attributed to the presence of pyrrhotite (Dekkers 1989b; Jackson *et al.* 1993), although such a feature might also be the combined effect of the Verwey transition and the presence of goethite.

In none of the haematite-bearing lithologies (e.g. PLE1-4, Fig. 2d) a significant change in magnetization occurs at the haematite transition temperature (Morin transition, *ca* 255–265 K). However, the Morin transition is very sensitive to the incorporation of impurities in the haematite crystal lattice and is suppressed by small amounts (e.g. 1 atom per cent Ti substitution) of foreign-ion substitution (Morrish 1994, and references therein). The temperature and height of the Morin transition also depend on the particle size; it is completely absent in haematite grains with diameters less than ∼0.02 μm (Bando *et al.* 1965).

4.4 Hysteresis measurements

Prior to interpretation, the hysteresis loops were corrected for paramagnetic or diamagnetic components. Biohermal carbonate rocks (GRU1, Fig. 3a) have wasp-waisted hysteresis loops (Roberts *et al.* 1995) and the diamagnetic signal outweighs the contribution from paramagnetic minerals. Platform carbonate rocks contain more paramagnetic material and the hysteresis loops are less constricted at low fields compared with biohermal carbonate rocks (HAC2-2, Fig. 3b). Loops from clastic lithologies are not wasp waisted and show a strong paramagnetic signal (ALB1GM, BRU1-6, Figs 3c and d). The misfit between the individual hysteresis branches at high fields in Figs 3(c) and (d) is a result of the large amount of paramagnetic material and a small systematic temperature change of the sample during measurement. Samples from red beds (site PLE) and from rocks where the Triassic remagnetization component was identified (sites ATT1 and ATT2) do not reach saturation during hysteresis measurements (ATT2-5, Fig. 3e). Here, the constricted loops indicate the presence of both a high- and low-coercivity phase, which are thought to be haematite and magnetite. Fig. 4 shows the hysteresis ratios M_{rs}/M_s and H_{cr}/H_c of samples from different groups of lithologies, where high-coercivity minerals such as haematite and goethite are absent. Samples, where thermal demagnetiz4ation of a triaxial IRM and/or low-temperature behaviour indicate the presence of small amounts of pyrrhotite are indicated with open symbols in Fig. 4.

The hysteresis ratios of the magnetite-bearing sedimentary rocks display a distinct relation to lithology. Samples from biohermal carbonate rocks (diamonds in Fig. 4) have characteristically high hysteresis ratios, which fall on the mixing line [$M_{rs}/M_s = 0.89\,(H_{cr}/H_c)^{-0.6}$; line b in Fig. 4], observed by Jackson (1990) in remagnetized carbonate rocks from North America. The hysteresis ratios of most clastic rocks fall on the mixing line of SD and MD magnetite (Parry 1982; line a in Fig. 4). Here, the high values of H_{cr}/H_c and low values of M_{rs}/M_s indicate the predominance of MD magnetite. The platform carbonate rocks (triangles in Fig. 4) and some fine grained clastic rocks (siltstones) have higher hysteresis ratios than SD–MD mixtures and fall between the two groups described above (line c in Fig. 4). This relation between the hysteresis ratio and lithology is also observed in samples where IRM demagnetization and low temperature measurements indicate that magnetite is accompanied by small amounts of pyrrhotite (open symbols in Fig. 4; sample BOH1-5B from Fig. 1d is not included here).

4.5 Viscosity and frequency dependence of susceptibility

The viscous decay of an IRM (1 T at 300 K) was observed for 290 s. The remanence decreases between 2 and 7 per cent during the experiments in samples from all lithologies (Fig. 5a). This decay is caused by thermally activated domain wall jumps in MD particles or by grains just above the SP size that have relaxation times in the order of tens of seconds (Dunlop & Özdemir 1997) and is described by the magnetic viscosity coefficient $S = |(\partial M/\partial \log t)|$, normalized by the initial remanence M_r (10 s). The normalized magnetic viscosity coefficients of rocks, in which the Late Carboniferous remagnetization was identified, seem to be controlled by lithology (Fig. 5b). The viscosity coefficient of most carbonate rocks (e.g. GRU1 in

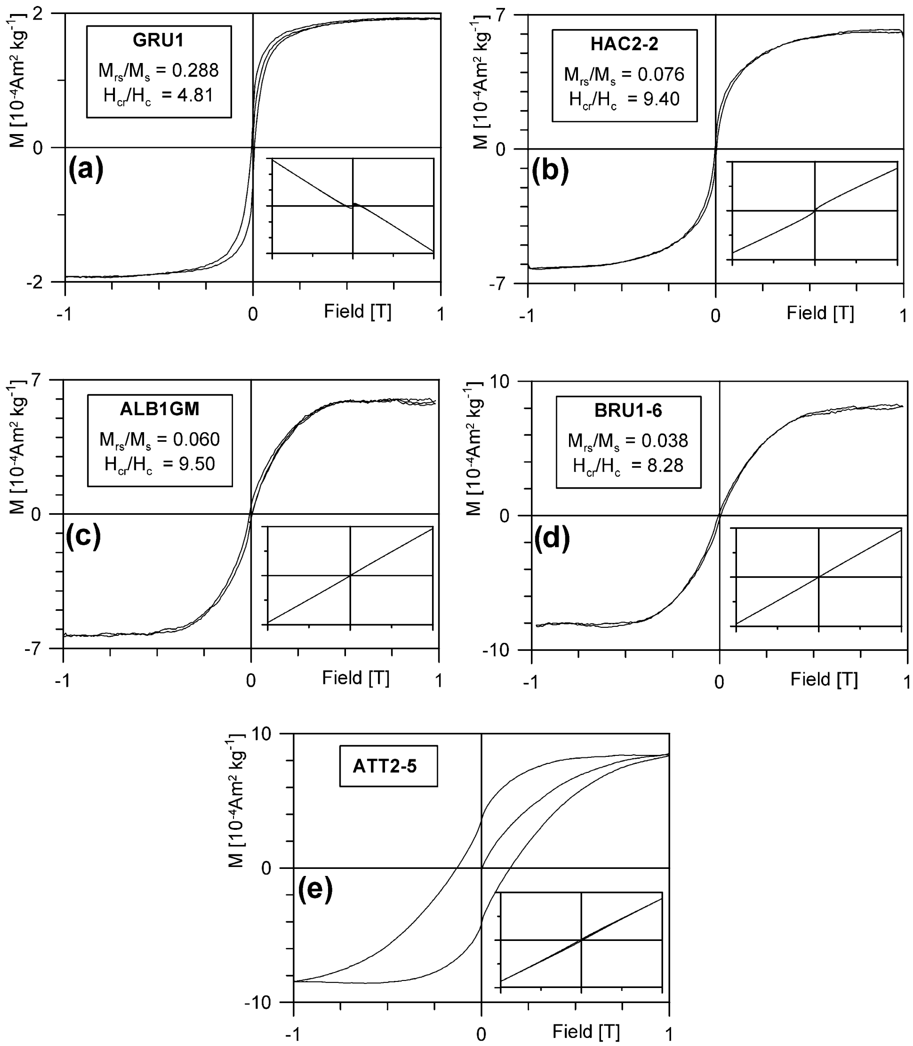

Figure 3. Hysteresis loops of samples from (a) biohermal carbonate rocks (GRU1), (b) platform carbonate rocks (HAC2-2), (c) siltstones (ALB1GM), (d) quartzwackes (BRU1-6) and (e) red calcareous siltstones (ATT2-5). Loops of carbonate rocks are often wasp waisted (GRU1, HAC2-2), whereas the siliciclastic rocks are characterized by very slim loops (ALB1GM, BRU1-6). Samples from red lithologies (red beds or red calcareous siltstones) do not reach saturation during hysteresis measurements (ATT2-5). The hysteresis curves are constricted at low fields, indicating the presence of high- and low-coercivity phases, which are thought to be haematite and magnetite. The insets show the original shape of the hysteresis loops before correction for diamagnetism (GRU1) and paramagnetism (all other samples).

Fig. 5a) varies between 0.025 and 0.03 s^{-1} and is higher than for the majority of clastic rocks (*ca* 0.01–0.02 s^{-1}, e.g. LOS3-4 in Fig. 5a). The observation of a higher magnetic viscosity in lithologies with few or no amounts of MD magnetite indicates a significant contribution from SP magnetite. Haematite-bearing samples, in which the Triassic remagnetization was identified, have viscosity coefficients between 0.02 and 0.025 s^{-1} (Table 1).

A significant change (4–8 per cent) in susceptibility during frequency sweeps from 40 to 4000 Hz (AC field: 200 Am^{-1}) at room temperature was observed only for platform carbonate and a few siliciclastic rocks. Although the bulk susceptibilities of the clastic samples are relatively high (10^{-3} to 10^{-5} SI), the relative changes with frequency were mostly below the sensitivity of the Lakeshore susceptometer, which was estimated by repeated measurements of a paramagnetic material (Gd_2O_3). The small frequency dependence of the siliciclastic rocks is thought to result from a very small contribution of SP material to the bulk susceptibility, which is dominated by paramagnetic minerals (e.g. micas, Fe-chlorite) and MD magnetite. This is also reflected by a low ratio of ferromagnetic to paramagnetic susceptibility of less than 5 per cent.

5 DISCUSSION

The remagnetized rocks from the NE Rhenish massif yield a wide spectrum of rock magnetic properties and are characterized by a complex magnetomineralogy.

Magnetite is identified in all lithologies and is the dominant carrier of the Late Palaeozoic remagnetization. The appearance of the Verwey transition, which is evident in clastic rocks but suppressed or absent in carbonate rocks, indicates decreasing amounts of MD magnetite of detrital origin in siliciclastic rocks, platform carbonate rocks and biohermal carbonate rocks. This is supported by the ratio M_{rs}/M_s, plotted versus H_{cr}/H_c (Fig. 4), which is typical for SD–SP magnetite for biohermal carbonate rocks and typical for SD–MD mixtures for clastic rocks, with intermediate values for platform carbonate rocks. The different lithologies

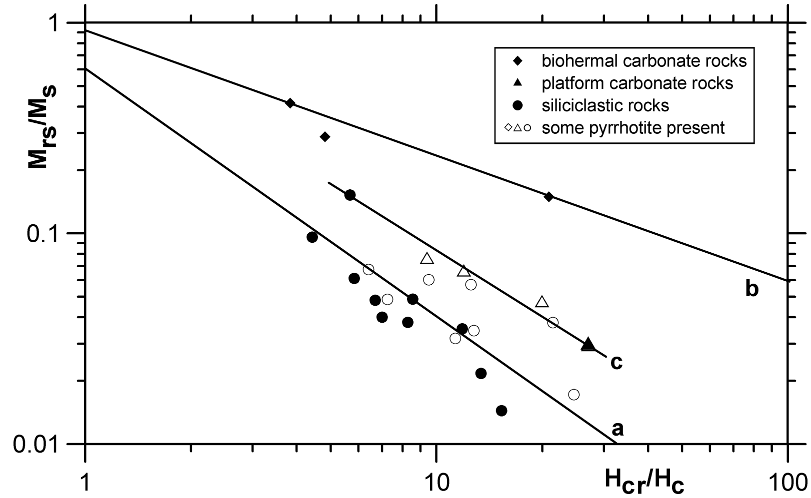

Figure 4. Plot of the hysteresis ratios M_{rs}/M_s and H_{cr}/H_c. The majority of siliciclastic rocks (circles) fall on the SD–MD mixing line after Parry (1982, line a), whereas reef carbonates (diamonds) have hysteresis properties similar to those obtained from North American remagnetized carbonates (Jackson 1990, line b). Fine grained clastic rocks and platform carbonates (triangles) fall in between both groups described above (line c). Samples, where a small contribution from pyrrhotite was observed during thermal demagnetization of a triaxial IRM and cooling of an IRM_{RT} (open symbols), show a similar relation between lithology and hysteresis ratios.

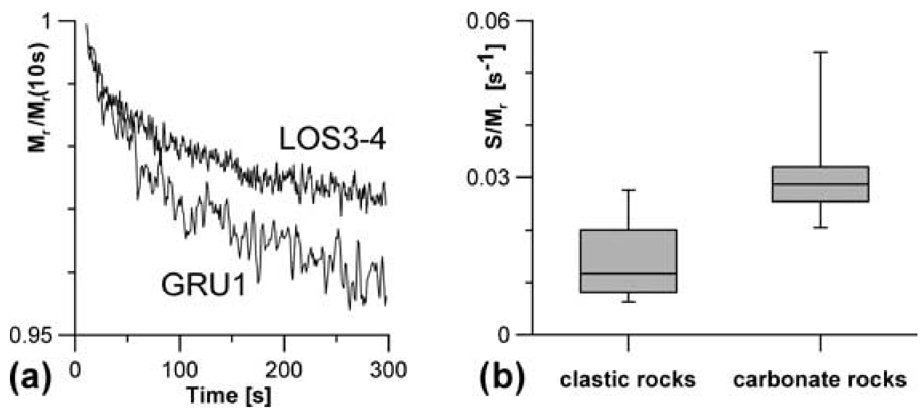

Figure 5. (a) Viscous decay of an IRM (1 T) for two samples from biohermal carbonate rocks (GRU1) and quartzwackes (LOS3-4); (b) median (horizontal line), range of mean 50 per cent of results (shaded boxes) and extreme values (caps) of the normalized magnetic viscosity coefficient for clastic and carbonate rocks, in which the Late Carboniferous remagnetization was identified.

studied here can be discriminated in a plot of M_{rs}/M_s against the relative change in magnetization of the zero field heating curve across the Verwey transition (δ_{ZFC}) shown in Fig. 6. The trend from high M_{rs}/M_s and a weak Verwey transition in biohermal carbonate rocks to low M_{rs}/M_s and a distinct Verwey transition in siliciclastic rock reflects an increasing contribution from detrital MD magnetite.

Because the amount of MD magnetite and paramagnetic material is low in carbonate rocks, their rock magnetic properties (zero field heating curve decrease between 20–100 K, k_{fd}, S/M_r and hysteresis parameters) are indicative of the presence of SP material. In particular, the relatively high magnetic viscosity and high hysteresis ratios in the carbonate rocks (see Fig. 4) evidence the existence of ultrafine (SP) grained magnetic material with relaxation times in the order of tens of seconds or below. Biohermal carbonate rocks have hysteresis ratios that correlate with values reported by Jackson (1990) for remagnetized carbonate rocks from the North American Hercynian fold belt.

The high detrital input of the siliciclastic rocks is reflected in low hysteresis ratios and in a high paramagnetic susceptibility, which are indicative of a large amount of MD magnetite and paramagnetic silicate minerals, respectively. Instead of being indicative of the presence of SP magnetite, the decrease in zero field heating curves between 10 and 100 K in those rocks could be caused by paramagnetic minerals, which magnetically order at very low temperatures. The magnetic viscosity in the siliciclastic rocks might result from the movement of domain walls in MD magnetite, rather than viscous unblocking of magnetite, close to the SP–SD grain size threshold. Consequently, the massive contribution of paramagnetic minerals and MD magnetite to the rock magnetic properties of the siliciclastic rocks disguises any possible contribution from ultrafine grained material.

The hysteresis properties of platform carbonate rocks and some fine grained clastic rocks (siltstones) fall between the values of the lithologies described above. Their hysteresis ratios are lower than those of the biohermal carbonate rocks and higher than those of most siliciclastic rocks and pure MD–SD magnetite mixtures. Compared with siliciclastic rocks, terrigenous material is less abundant in platform carbonate rocks. Therefore, the amount (and total volume) of magnetite grains above the SD–MD boundary is expected to be smaller. The observation of intermediate hysteresis results in those

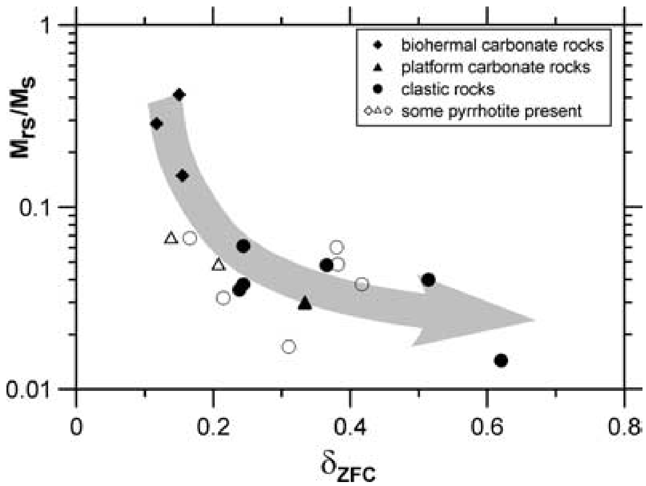

Figure 6. The ratio $M_{\mathrm{rs}}/M_{\mathrm{s}}$ plotted against the intensity decay across the Verwey transition during heating of an $\mathrm{IRM}_{\mathrm{LT}}$ in zero field $\{\delta_{\mathrm{ZFC}} = [\mathrm{M(100\ K)\text{-}M(130\ K)}]/\mathrm{M(100\ K)}\}$. The arrow indicates the trend of increasing amounts of MD magnetite with decreasing $M_{\mathrm{rs}}/M_{\mathrm{s}}$ and increasing size of the Verwey transition.

rocks indicates the coexistence of two generations of magnetite in the sedimentary rocks of the NE Rhenish massif: (i) detrital magnetite, predominantly in MD state and (ii) authigenic mixtures of SD magnetite dominated by magnetocrystalline anisotropy and ultrafine (SP) magnetite. Based on the observation of intermediate hysteresis results in some fine grained siliciclastic rocks, it seems reasonable to predict the existence of the authigenic magnetite generation in the clastic rocks in general, although it is often disguised by MD magnetite.

The absence of MD magnetite in the biohermal carbonate rocks is thought to rule out anomalously high T_{ub} of the NRM caused by MD remanence (e.g. Dunlop *et al.* 1997). This supports the interpretation of Zwing *et al.* (2002), that the thermal stability of the Late Carboniferous remanence (up to 550 °C) is in contradiction with a thermoviscous remagnetization.

The thermal demagnetization behaviour of the NRM indicates, that pyrrhotite and haematite can accompany magnetite as a carrier of the Late Carboniferous remagnetization (Zwing *et al.* 2002). The occurrence of pyrrhotite is supported by the thermal demagnetization pattern of a triaxial IRM and the observations of the low-temperature transition of pyrrhotite at 32 K during the low-temperature experiments. Pyrrhotite is identified in platform carbonate and siliciclastic rocks and its occurrence seems to be related to the presence of organic matter (e.g. bituminous biomicrites from site HAC, see Table 1), which indicates anoxic or suboxic conditions during sedimentation and diagenesis. In most biohermal carbonate rocks, pyrrhotite is absent. This suggests that the particular high hysteresis ratios of carbonate rocks in the NE Rhenish massif are not caused by mixtures of magnetite and pyrrhotite, which might be responsible for similar hysteresis results in some remagnetized carbonate rocks from North America (Jackson *et al.* 1993).

Haematite is identified during thermal demagnetization of the triaxial IRM in Early Devonian red beds (site PLE) carrying the Late Carboniferous remagnetization and in Late Devonian quartzarenites (ATT1) and calcareous siltstones (ATT2), where the Triassic overprint was identified. Although thermal demagnetization of a triaxial IRM indicate high amounts of haematite in those rocks (Fig. 1e), the Morin transition was never observed during the low-temperature experiments and is thought to be suppressed by very small particle sizes and small amounts of foreign-ion substitution. The behaviour during hysteresis, IRM demagnetization and low temperature experiments of both groups of haematite-bearing samples is quite similar, except for higher magnetic viscosity coefficients of samples, which carry the Triassic magnetic component (Table 1). Thermal demagnetization of a triaxial IRM of those rocks confirms the presence relatively large amounts of magnetite, compared with the other lithologies studied (*ca* 2–8 times more than in other siliciclastic rocks). Therefore, the viscosity of rocks carrying the Triassic overprint (component C) could be caused by SP or MD magnetite, rather than by haematite.

Goethite occurs in some carbonate rocks and is best identified by an intensity decrease in IRM (high-coercivity component) below 150 °C. In most cases, goethite carries an NRM with a direction similar to the present day field direction and is thought to result from oxidation of sulphides (pyrite, pyrrhotite) during weathering.

6 CONCLUSION

The rock magnetic experiments yield a complex magnetomineralogy of the remagnetized palaeozoic sedimentary rocks (biohermal carbonate rocks, platform carbonate rocks, siliciclastic rocks) from the NE Rhenish massif and support the interpretation of NRM demagnetization data (Zwing *et al.* 2002). The most important carrier of the late Palaeozoic magnetization component is magnetite, but haematite and pyrrhotite can accompany magnetite as carriers of the Late Carboniferous remagnetization in red beds (haematite) and in lithologies, where with anoxic to suboxic conditions prevailed (pyrrhotite).

The magnetic viscosity and low-temperature behaviour of carbonate rocks give strong evidence for the presence of ultrafine (SP) magnetite. This material is also thought to be partly responsible for the magnetic viscosity and low-temperature behaviour of siliciclastic rocks. This interpretation, however, is not unique for the siliciclastic rocks, as a result of the predominance of detrital MD magnetite and the high amount of paramagnetic material.

The hysteresis ratios from most siliciclastic rocks and biohermal carbonate rocks fall in or close to the fields of MD magnetite (Parry 1982) and remagnetized carbonate rocks (Jackson 1990), respectively. Some fine grained clastic rocks (siltstones) and platform carbonate rocks have hysteresis properties between those of reef carbonate rocks and coarse siliciclastic rocks. This points towards the presence of ultrafine grained magnetic material in all lithologies. However, its magnetic fingerprint gets increasingly disguised with increasing amounts of detrital MD magnetite. This implies that hysteresis ratios can only be applied to detect remagnetizations for lithologies where MD magnetite is subsidiary or absent.

The low palaeotemperatures and high unblocking temperatures of the remagnetization component disagree with a thermal remagnetization event in the NE Rhenish massif (Zwing *et al.* 2002). The new rock magnetic results, indicating the presence of ultrafine grained magnetic material in carbonate and clastic rocks give further evidence for a chemical remagnetization process in this region. Whether the growth of magnetic minerals was controlled by the migration of fluids, by the break-up of Fe-rich smectite during burial diagenesis or by any other mechanism has yet to be shown.

ACKNOWLEDGMENTS

We thank Mark Dekkers and an anonymous reviewer for helpful comments. Most of the measurements were conducted at the

Institute for Rock Magnetism and we would like to thank Mike Jackson, Jim Marvin and Pete Solheid for their support. Funding for the Institute for Rock Magnetism is provided by the W. M. Keck Foundation, the National Science Foundation and the University of Minnesota. AZ acknowledges a visiting fellowship from the Institute for Rock Magnetism. This research was funded by the Deutsche Forschungsgemeinschaft (DFG).

REFERENCES

Bando, Y., Kiyama, M., Yamamoto, N., Takada, T., Shinjo, T. & Takaki, H., 1965. Magnetic properties of alpha-Fe2O3 fine particles, *J. Phys. Soc. Japan,* **20,** 2086.

Coey, J.M.D., 1988. Magnetic properties of iron in soil iron oxides and clay minerals, in *Iron in soils and clay minerals,* pp. 397–466, eds Stucko, J.W., Goodman, B.A. & Schwertman, U., D. Reidel Publishing Company, Dordrecht–Boston.

Dekkers, M.J., 1988. Magnetic properties of natural pyrrhotite Part I: Behaviour of initial susceptibility and saturation-magnetization-related rock-magnetic parameters in a grain-size dependent framework, *Phys. Earth planet. Int.,* **52,** 376–393.

Dekkers, M.J., 1989a. Magnetic properties of natural goethite—II. TRM behaviour during thermal and alternating field demagnetization and low-temperature treatment, *Geophys. J.,* **97,** 341–355.

Dekkers, M.J., 1989b. Magnetic properties of natural pyrrhotite, Part II: High- and low-temperature behaviour of Jrs and TRM as a function of grain size, *Earth planet. Sci. Lett.,* **57,** 266–283.

Dunlop, D.J. & Özdemir, Ö., 1997. *Rock magnetism: fundamentals and frontiers,* Cambride University Press, Cambridge, p. 573.

Dunlop, D.J., Özdemir, Ö. & Schmidt, P.W., 1997. Paleomagnetism and paleothermometry of the Sydney Basin. 2. Origin of anomalously high blocking temperatures, *J. geophys. Res.,* **102,** 27 285–27 295.

Elmore, R.D., London, D., Bagley, D., Fruit, D.J. & Gao, G., 1993. Remagnetization by basinal fluids; testing the hypothesis in the Viola Limestone, southern Oklahoma, *J. geophys. Res.,* **98,** 6237–6254.

Folk, R.L., 1957. *Petrology of sedimentary rocks,* Hemphill, Austin, p. 111.

Franke, W., 2000. The mid-European segment of the Variscides: tectonostratigraphic units, terrane boundaries and plate tectonic evolution, in *Orogenic Processes: Quantification and Modelling in the Variscan Belt,* Special Publications 179, 35–61, eds Franke, W. *et al.*, Geological Society of London, London.

Jackson, M., 1990. Diagenetic source of stable remanence in remagnetized paleozoic cratonic carbonates: a rock magnetic study, *J. geophys. Res.,* **95,** 2753–2761.

Jackson, M., Rochette, P., Fillion, G., Banerjee, S.K. & Marvin, J., 1993. Rock magnetism of remagnetized Paleozoic carbonates; low-temperature behaviour and susceptibility characteristics, *J. geophys. Res.,* **98,** 6217–6225.

Königshof, P., 1992. Der Farbänderungsindex von Conodonten (CAI) in paläozoischen Gesteinen (Mitteldevon bis Unterkarbon) des Rheinischen Schiefergebirges, *Cour. Forsch.-Inst Senckenberg,* **146,** 1-118.

Lowrie, W., 1990. Identification of ferromagnetic minerals in a rock by coercivity and unblocking temperature properties, *Geophy. Res. Lett.,* **17,** 159–162.

McCabe, C. & Channell, J.E.T., 1994. Late Paleozoic remagnetization in limestones of the Craven Basin (northern England) and the rock magnetic fingerprint of remagnetized sedimentary carbonates, *J. geophys. Res.,* **99,** 4603–4612.

McCabe, C. & Elmore, R.D., 1989. The occurence and origin of late paleozoic remagnetizations in the sedimentary rocks of North America, *Rev. Geophys.,* **27,** 471–494.

Molina Garza, R.S. & Zijderveld, J.D.A., 1996. Paleomagnetism of Paleozoic strata, Brabant and Ardennes massifs, Belgium; implications of prefolding and postfolding Late Carboniferous secondary magnetizations for European apparent polar wander, *J. geophys. Res.,* **101,** 15 799–15 818.

Morrish, A.H., 1994. *Canted antiferromagnetism: Hematite,* World Scientific, London, p. 192.

Özdemir, Ö., Dunlop, D.J. & Moskowitz, B.M., 1993. The effect of oxidation on the Verwey transition in magnetite, *Geophy. Res. Lett.,* **20,** 1671–1674.

Paproth, E. & Wolf, M., 1973. Zur paläogeographischen Deutung der Inkohlung im Devon und Karbon des nördlichen Rheinischen Schiefergebirges, *N. Jahrb. Geol. Paläo. Mh.,* **8,** 469–493.

Parry, L.G., 1982. Magnetization of immobilized particle dispersions with two distinct particle sizes, *Phys. Earth planet. Int.,* **28,** 230–241.

Pettijohn, F.J., Potter, P.E. & Siever, R., 1973. *Sand and Sandstone,* Springer, Berlin, p. 617.

Roberts, A.P., Chui, Y. & Verosub, K.L., 1995. Wasp-waisted hysteresis loops: Mineral magnetic characteristics and discrimination of components in mixed magnetic systems, *J. geophys. Res.,* **100,** 17 909–17 924.

Stamatakos, J., Hirt, A.M. & Lowrie, W., 1996. The age and timing of folding in the Central Appalachians from paleomagnetic results, *Bull. geol. soc. Am.,* **108,** 815–829.

Suk, D., Van der Voo, R. & Peacor, D.R., 1991. SEM/STEM observations of magnetite in carbonates of Eastern North America: evidence for chemical remagnetization during the Alleghenian Orogeny, *Geophys. Res. Lett.,* **18,** 939–942.

Suk, D., Van der Voo, R. & Peacor, D.R., 1993. Origin of magnetite responsible for remagnetization of early Paleozoic limestones of New York State, *J. geophys. Res.,* **98,** 419–434.

Walliser, O.H., 1981. The geosynclinal development of the Rheinische Schiefergebirge (Rhenohercynian zone of the Variscides; Germany), *Geol Mijnbouw,* **60,** 89–96.

Xu, W., Van der Voo, R. & Peacor, D.R., 1994. Are magnetite spherules capable of carrying stable magnetizations?, *Geophys. Res. Lett.,* **21,** 517–520.

Zegers, T.E., Dekkers, M.J. & Bailly, S., 2003. Late Carboniferous to Permian remagnetization of Devonian limestones in the Ardennes: Role of temperature, fluids, and deformation, *J. geophys. Res.,* **108,** 2357, doi:10.1029/2002JB002213.

Zwing, A., Bachtadse, V. & Soffel, H.C., 2002. Late Carboniferous Remagnetisation of Palaeozoic Rocks in the NE Rhenish Massif, Germany, *Phys. Chem. Earth,* **27,** 1179–1188.